Simulation of the Position Control of PAM, Using Its' Nonlinear Dynamic Model

István Bíró[1], Monika Trojanová[2], Tomáš Čakurda[2], Zoltán Fabulya[3] and József Sárosi[4]

Department of Mechanical Engineering, Faculty of Engineering, University of Szeged, Mars tér 7, 6724 Szeged, Hungary, biro-i@mk.u-szeged.hu

Department of Industrial Engineering and Informatics, Faculty of Manufacturing Technologies with a Seat in Prešov, Technical University of Košice, 1 Bayerova, 080 01 Prešov, Slovakia; monika.trojanova@tuke.sk; tomas.cakurda@tuke.sk

Department of Engineering Management and Economics, Faculty of Engineering, University of Szeged, Mars tér 7, 6724 Szeged, Hungary, fabulya@mk.u-szeged.hu

Department of Mechatronics and Automation, Faculty of Engineering, University of Szeged, Moszkvai krt. 9, 6725 Szeged, Hungary, sarosi@mk.u-szeged.hu

Abstract: The paper investigates the mathematical, dynamic nonlinear model, of a single Pneumatic Artificial Muscle (PAM). A Fluid muscle from FESTO, is connected vertically as an oscillating non-linear system with 1 degree of freedom. When the muscle is filled with a working medium - compressed air, there is a change in the pressure over time and muscle parameters (change in length, diameter, fiber braiding angle, mass position, etc.). The simulation of the position of mass is the goal of the research described in this article. A mathematical model of the system, considers the change in the spring stiffness and the damping factor. At the same time, the model considers the effect of time pressure changes, on system oscillation. The article provides a few examples, which help specify the positioning model (also identifying values of individual coefficients of quantities occurring in the model).

Keywords: pneumatic artificial muscle (PAM); nonlinear dynamic model; oscillator; positioning; mathematical model

1 Introduction

For robots and manipulators, it is necessary to note several attributes, that should be ensured, for proper functioning: manipulation, automation, programmability, universality, feedback, and others. The importance of the individual properties results from their use. Properties are influenced by the elements, such as design,

actuators, sensors, and control [1]. In addition to conventional types of robotic actuators (e.g., electric or hydraulic), many researchers have also focused on unconventional types, e.g., pneumatic artificial muscle (see. [2-6]). It is a device that consists of two layers and endings, whose task is to generate tensile force after filling the muscle with the working media. Around 1930, the first researcher of the Pneumatic Artificial Muscle (Garasiev) focused mainly on constructing the muscle. His muscle, however, encountered the problem of inadequate material technology, whereby the fibers were unable to produce sufficient elasticity. At present, the most typical representative of this type of actuator - McKibben's artificial muscle, is characterized by softness, flexibility, easy maintenance, and possible use in demanding operating conditions, which can be a significant benefit also for industrial applications. Due to the friction between fibers themselves or between the fibers and tube, its behavior is nonlinear and hysteretic. This deficiency was addressed by FESTO [7], which combined the inner and outer layers in one, thereby prolonging the lifetime of the muscle compared to other muscles and improving its performance. Although the manufacturer has eliminated some undesirable properties, it is still necessary to consider the occurring hysteresis and nonlinearity of the characteristics that make the identification process more difficult.

Identification allows analyzing relationships and processes within the system and creates a model representing this system. Proper positioning of PAM-powered systems is also subject to the process of modeling pneumatic artificial muscles, which is the subject of the research described not only in this article but also by other researchers in the field. Studies by experts in PAM include, e.g., studies of the mechanical properties of PAM described in [8]. These are experimental models describing the mechanics of the behavior of PAM, where the experiment is performed at three different muscle sizes and different loads. Another study describes progress in PAM research [9]. The authors summarized an overview of artificial muscles, artificial muscle division, application of artificial muscles, but at the same time described a study of the control of the artificial muscle algorithm (similar as in the introduction of reference [10]).

Some approaches are currently known for modeling pneumatic artificial muscles. E.g., in [11] is an overview of the commonly used techniques to modeling pneumatic artificial muscles. The most used approach to modeling is experimental. It was used, e.g., in [8, 12-16]. In [17] is experimentally characterize the behavior of McKibben's muscles. The model can predict muscle displacement and force parameters under static conditions. Comparing the measured data with the model showed the model's ability to predict static characteristics. Similarly, [18] describing a 2-muscle FESTO test device. Authors also describe methods used to determine muscle characteristics under static conditions (isobaric, isometric, and isotonic). The measured data from the experimental device were used for the analytical determination of equations of characteristics, which were subsequently used for the simulation of characteristics. An experimental modeling approach is not always practical. In that case, is chosen the analytical method of finding the

solution (especially searching for the analytical model based on the measured values). In [19] is an analytical static model based on Newton mechanics, comparing the model results with the measured data. One of the latest publications in analytical modeling of systems powered by PAMs is [20]. It describes a nonlinear numerical approximation of non-linear static characteristics of the McKibben PAM (namely the dependence of force on deformation and pressure), the output of which are four mutually compared functions. Models and publications that describe the system's dynamics are more time-consuming in terms of research and preparation. The reason is perhaps the occurrence of non-linear characteristics and the higher number of elements in the system. This fact complains about the process of identifying the model under dynamic conditions. However, [21] describes a dynamic model for a system with 2 degrees of freedom, where the nonlinearity of the force-dependent on muscle pressure and deformation is investigated. The force parameter was obtained analytically, followed by experimental testing. [22] describes the creation of dynamic models whose role is to accurately predict the dynamic behavior of muscles. The dynamic model is simulated using the Matlab, and the pressure, contraction, and muscle temperature are tested experimentally. The most recent article describing a 1 degree of freedom system, to derive a motion equation from studying resonant conditions is [23]. This paper derives a nonlinear motion control equation concerning muscle strength as a function of pressure (both static and time-variable).

The monitoring of hysteresis and nonlinearity of the characteristics of pneumatic artificial muscles plays an essential role in achieving the highest possible level of system identification and, consequently, control. E.g., in [24] is described motion control of manipulator that have 2 degrees of freedom. The manipulator is parallel and uses 3 PAMs. Because the authors realize the relationship between muscle pressure and contraction rate, they included a hysteresis characteristic in their research. Therefore, they tried to design a control system with integrated hysteresis compensation. Ref. [25] describes the dependence of friction by speed, the dependence of coefficient friction by pressure, and hysteresis itself. Also, [26] describes a static force model for a hysteresis loop in a force-contraction curve, and it has also been experimentally verified. Modeling and hysteresis compensation is also research in [27], where a generalized Bouc-Wen model is applied for dynamic modeling of hysteresis. Finally, in the literature [28], the authors present new equations for modeling the length of contraction using the sigmoid shape of the characteristics.

There is an enormous amount of applied research where pneumatic artificial muscles are integrated into the purpose-built device. Their application is diverse (from industry in the medical field of prostheses to applications in everyday life). E.g., authors in [29] describe the application of flexible fluidic actuators to grippers or arms. Another applied research is the project, which in [30] presents the design and construction of an electro-pneumatic parallel manipulator with 3 degrees of freedom allows to pick up objects in recycled waste facilities. The last applied

research is active bridge vibration control, which is stretched by pneumatic artificial muscles [31]. The task of the researchers was first to derive a discrete analytical model, which was subsequently verified by non-feedback experiments. Then, based on the model, a feedback control model was designed.

The research described in the article aims to use a nonlinear dynamic model in simulations of position control of the pneumatic artificial muscle. The model can respond to spring stiffness and damping factor changes depending on the muscle contraction (eliminating muscle mass oscillations). A fluidic muscle DMSP-20-400 N with the length of 400 mm and diameter of 20 mm was therefore chosen for the experiments. The individual parts of the article contain the process of derivation of the mathematical model of the system, which considers the change in muscle stiffness and contraction-dependent damping, is described. Finally, the research results are presented on examples of the muscle reaching a specific state at selected coefficients that influence the resulting oscillation.

2 Nonlinear Dynamic Model of the Pneumatic Artificial Muscle

Suppose the pneumatic artificial muscle is connected so that one end is firmly attached and a load with a certain weight m is placed at the other end. In that case, if the muscle is filled with a working medium, a contraction will occur, and the load will be pulled upwards. The muscle thus has one degree of freedom. The pneumatic artificial muscle can accordingly be modeled as an oscillator. The vibration model is shown in Figure 1 (m is mass of the load, x is displacement, g is the acceleration of gravity, c is coefficient of damping, k is stiffness, and F_{spring} is contractile force developed by PAM).

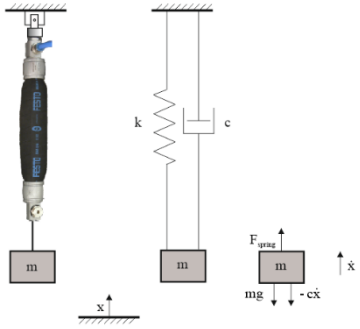

Figure 1
Oscillator formed by a pneumatic artificial muscle and one degree of freedom

In the spring-mass system, where damping is also present, vibrations occur due to a non-linear force, and at the same time, a gravitational force is present in a

vertically downward direction. Its vibration can be described by the following second-order differential equation:

$$m\ddot{x} = F_{spring} - mg - c\dot{x} \tag{1}$$

2.1. Contractile Force F_{spring}

The dimension of the contractile force produced in PAM depends on the parameters of the muscle, namely: the material from which the inner and outer muscle layers are made; geometric parameters of the fibers of these layers; and the pressure of the working medium in the muscle – the applied pressure of the air.

The contractile force is closely related to an important muscle property - contraction. Muscle contraction is the relative displacement with initial length l_0 of PAM and length l when the muscle is contracted. The equation for calculating muscle contraction is shown in Figure 2, which also indicates muscle parameters. While the muscle contraction is changing the length of the muscle, the angle of the muscle braid also changes from α_0 to α and the diameter of the muscle from d_o *to* d.

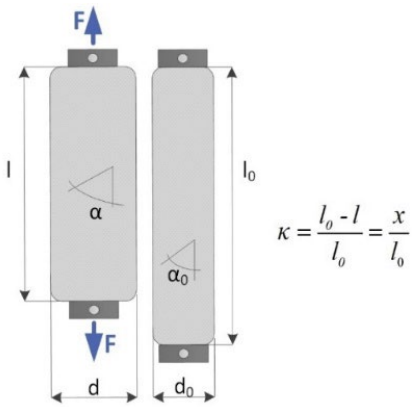

Figure 2
Contraction of pneumatic artificial muscle and its parameters

According to [21], F_{spring} contractile force can be described by an equation containing six unknown constants (a_1, a_2, a_3, a_4, a_5, and a_6) as follows:

$$F_{spring}(p,\kappa) = (a_1 \cdot p + a_2) \cdot exp^{a_3 \cdot \kappa} + a_4 \cdot \kappa \cdot p + a_5 \cdot p + a_6 \tag{2}$$

Where p is the gauge (applied), pressure and κ is a contraction.

It has to be noted that the damping coefficient depends on displacement for this reason, (1) can be rewritten into the following form:

$$m\ddot{x} = F_{spring}\big(\kappa(x)\big) - mg - c(\kappa(x))\dot{x} \tag{3}$$

The damping coefficient represents a nonlinear function of the displacement x. Therefore, to get values of $c(\kappa(x))$, it is needed to know the hysteresis based on force-contraction curves. Hysteresis occurs due to friction which occurs when a muscle contracts between individual muscle layers, layer fibers, or when muscle ends and layers touch.

2.2. Hysteresis of Force-Contraction Curves on Constant Pressures

In Figure 3, the scheme of the testbed for pressure, force, and position measuring is shown that consists of the following sensors and regulators: Motorola MPX5999D pressure sensor, LINIMIK MSA 320 incremental encoder, Kaliber 7923 load cell, and Festo VPPM-6L-L-1-G1/8-0L6H-V1N-S1C1 proportional pressure regulator (PPR). Acquisition and monitoring of measured data are developed in LabVIEW.

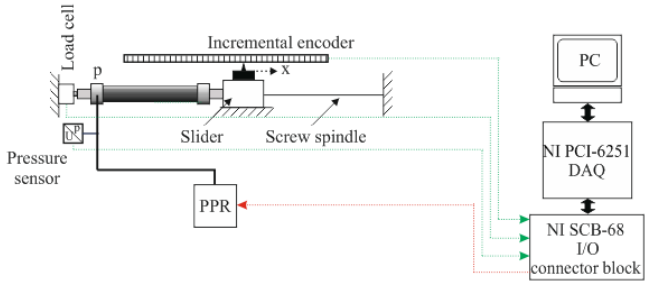

Figure 3

Experimental stand for measuring pressure, force, and position

Fluidic muscle type DMSP-20-400N is built into the rig. One of the ends of the muscle is fixed while the other is movable. The free end is connected to an incremental encoder (with a resolution of 0.01 mm) by a spindle. The list of technical parameters of fluidic muscle used in research is in the following table:

Table 1

List of technical parameters of DMSP 20-400N Festo fluidic muscle

Parameter	Value
Inside diameter	20 mm
Nominal length	400 mm
Maximal lifting force	1 500 N
Maximal operating pressure	600 kPa
Maximal permissible contraction	25 % of nominal length
Maximal permissible pretensioning	4 % of nominal length
Ideal temperature of the environment	from -5 °C to 60 °C

Firstly, the force-contraction function for various compressions is measured. The applied pressure is kept at a constant value while the screw spindle changes the length of PAM. Measuring at every point is repeated five times and statistically averaged. The hysteresis loop in the force-contraction curve is obtained when the procedure in the opposite direction is repeated. Approaching of experimentally measured hysteresis curves by Equation (2) is demonstrated in Figure 4. The figure shows that the function of static force and contraction depends on pressure. The maximum static force is reached by increasing the length of PAM. The zero-force is achieved at the minimum length of the muscle, i.e. at its maximum contraction. The muscle length is expressed in the figure in three basic positions. Nominal length - at zero muscle contraction. Minimal length - at maximum muscle contraction. Total length - presented as a negative contraction on the graph. Muscles from FESTO are made of durable but also flexible materials, which allow the muscle to have parameters such as Maximal permissible pretensioning and Maximal permissible contraction (it is possible to observe pre-tensioning in the muscle, based on which the contraction appears to be negative in the graph).

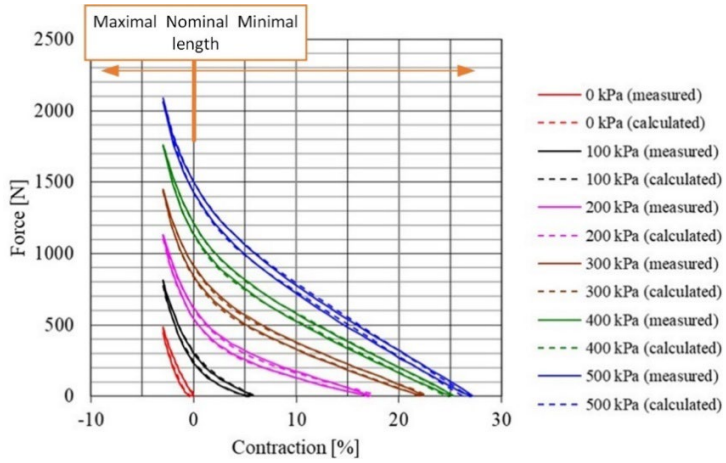

Figure 4

Hysteresis of force-contraction curves on constant pressures (measured and calculated by equation (2))

Figure 4 graphically presents the presence of hysteresis in the investigated system (PAM); therefore, it is necessary to optimize the branches of hysteresis based on Equation 2 (optimization of individual constants of Equation 2). Tables 2 and 3 contain results of optimization concerning the upper and lower branches of hysteresis. For upper branch $R^2 = 0.9995$ ($R = 0.9997$) as well as for the lower one $R^2 = 0.9991$ ($R = 0.9995$) accuracy are obtained.

Table 2

Parameters a_1, a_2, a_3, a_4, a_5, and a_6 of (2) for an upper branch of the hysteresis curve

Parameters	a_1	a_2	a_3	a_4	a_5	a_6
Values	-4.35573	281.22370	-0.32866	-9.27035	302.20107	-263.69185

Table 3
Parameters a_1, a_2, a_3, a_4, a_5, and a_6 of (2) for a lower branch of the hysteresis curve

Parameters	a_1	a_2	a_3	a_4	a_5	a_6
Values	3.65565	232.27984	-0.37855	-8.95540	290.68164	-277.50222

2.3. Damping Coefficient

The difference between one hysteresis surface (U_0 defines the area below the upper branch) and the other hysteresis surface (U_1 defines the area below the lower branch) is called the hysteresis surface ΔU ($\Delta U = U_0$-U_1). If the hysteresis surface ΔU and the surface under the upper branch U_0 are added, this ratio gives Lehr's damping coefficient. However, Lehr's damping coefficient can also be expressed as the ratio of the damping coefficient and the critical damping coefficient.

Based on the above, Lehr's damping coefficient can be written as

$$\zeta = \frac{\Delta U}{U_0} = \frac{c}{c_{cr}} \tag{4}$$

Subsequently, the critical damping coefficient c_{cr} can be given as

$$c_{cr} = 2 \cdot \sqrt{k \cdot m} \tag{5}$$

Where the stiffness k for constant pressure can be derived from (2) as:

$$k = k(\kappa) = \frac{dF(l)}{dl} = \frac{dF(\kappa)}{l_0 \cdot d\kappa} = \frac{1}{l_0} \cdot \frac{dF(\kappa)}{d\kappa} = \frac{1}{l_0} \cdot \frac{dF_{spring}(p,\kappa)}{d\kappa} =$$

$$= \frac{1}{l_0} \cdot \frac{d\left((a_1 \cdot p + a_2) \cdot exp^{a_3 \cdot \kappa} + a_4 \cdot \kappa \cdot p + a_5 \cdot p + a_6\right)}{d\kappa} = \frac{(a_1 \cdot p + a_2) \cdot a_3 \cdot exp^{a_3 \cdot \kappa} + a_4 \cdot p}{l_0} \tag{6}$$

The damping coefficient c can be given as

$$c = \zeta \cdot c_{cr} = \zeta \cdot 2 \cdot \sqrt{k \cdot m} = \zeta \cdot 2 \cdot \sqrt{\frac{m}{l_0} \cdot \left[(a_1 \cdot p + a_2) \cdot a_3 \cdot exp^{a_3 \cdot \kappa} + a_4 \cdot p\right]} \tag{7}$$

2.4. Dynamic Properties of PAM

Based on Figure 1 and (1), moving a load with a mass of 42 kg for a displacement of 72.0 mm at a pressure of 500 kPa, acceleration, velocity, displacement, and F_{spring} force as a function of time for the 1-DOF oscillatory system (described in Figure 1) can be seen in Figures 5-8. The functions were determined and created in Simulink.

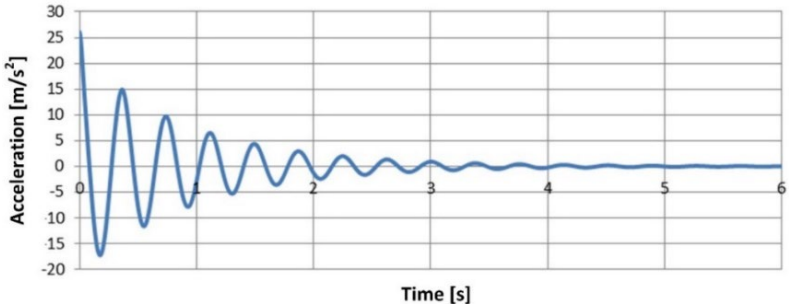

Figure 5
The acceleration-time function of the one-degree-of-freedom oscillatory system (pressure of 500 kPa, load of 42 kg, and displacement of 72.0 mm)

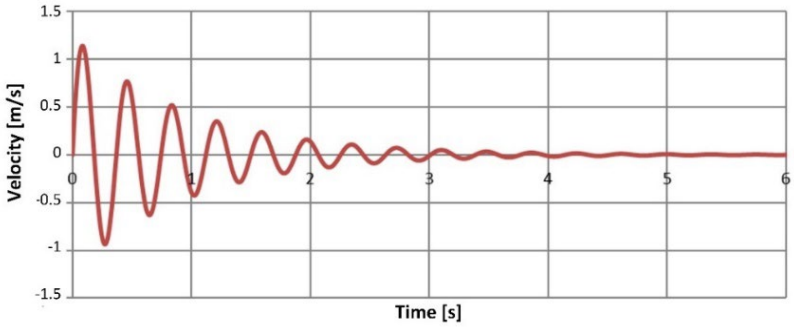

Figure 6
The velocity-time function of the one-degree-of-freedom oscillatory system (pressure of 500 kPa, load of 42 kg, and displacement of 72.0 mm)

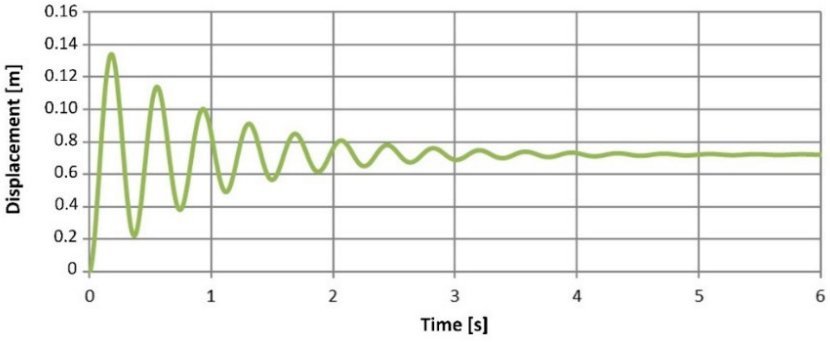

Figure 7
The displacement-time function of the one-degree-of-freedom oscillatory system (pressure of 500 kPa, load of 42 kg, and displacement of 72.0 mm)

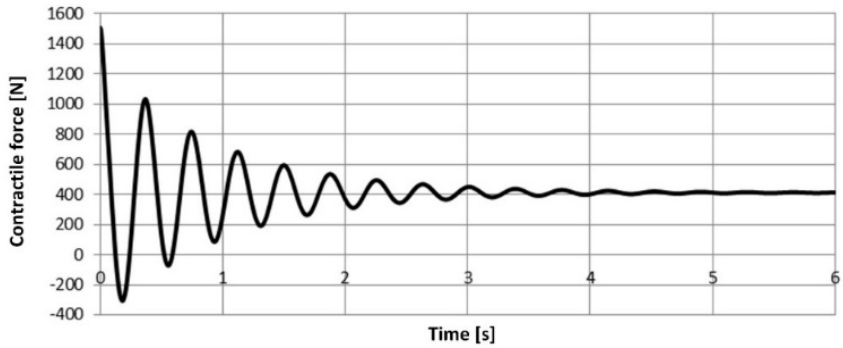

Figure 8

F_{spring} force-time function of the one-degree-of-freedom oscillatory system (pressure of 500 kPa, load of 42 kg, and displacement of 72.0 mm)

3 Nonlinear Dynamic Model of the Pneumatic Artificial Muscle Excited by Time-Varying Pressure

In the previous chapter of the article, Equation 3 was considered with respect to constant pressure. However, in case of taking into consideration the effect of variable pressure, the motion Equation (3) of the oscillating system in an upright position can be written down in the modified form:

$$m\ddot{x} - F_{spring}[\kappa(x), p(t)] + c[\kappa(x), p(t)]\dot{x} + mg = 0 \quad \text{or…}$$

$$m\ddot{x} - F_{spring}[\kappa(x), p((x(t))] + c[\kappa(x), p(x(t))]\dot{x} + mg = 0 \tag{8}$$

The second-order nonlinear differential Equation (8) can be solved solely in a numerical way. Applied algorithms to the initial value problem in MS Excel can be seen in Table 4 below.

Table 4

Applied algorithms in MS Excel for solving a differential equation

t	$\ddot{x}(\dot{x}, x)$	$\dot{x}$	x
t_o	$\ddot{x}_o(\dot{x}_o, x_o)$	$\dot{x}_o$	x_o
t_1	$\ddot{x}_1(\dot{x}_1, x_1)$	$\dot{x}_1 = \dot{x}_o + \ddot{x}_o(t_1 - t_o)$	$x_1 = x_o + \dot{x}_1(t_1 - t_o)$
t_2	$\ddot{x}_2(\dot{x}_2, x_2)$	$\dot{x}_2 = \dot{x}_1 + \ddot{x}_1(t_2 - t_1)$	$x_2 = x_1 + \dot{x}_2(t_2 - t_1)$
t_3	….	….	….
t_4	….	….	….

For example, there is a task to lift a mass m = 50 kg and keep its position on a level of 50 mm by applying a pneumatic artificial muscle. Then, at a pressure of 160 kPa, the motion in the vertical direction starts. According to Figure 9, the pressure in PAM has changed uniformly from 160 kPa to 400 kPa. Therefore, needed times in the investigated versions are 0 s, 0.1 s, 0.2 s, 0.3 s, and 0.4 s, respectively.

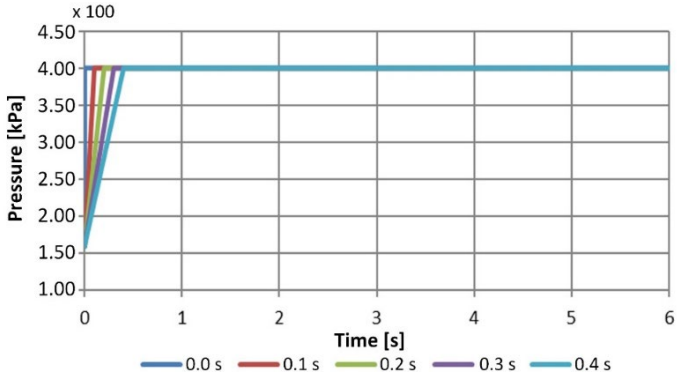

Figure 9
p(t) diagrams of PAM in case of different intensity of pressure ratio

In Figure 10, *x(t),* diagrams of PAM can be seen. In each case, the mass reaches the level of 50 mm (accurate value: 49.54 mm). To achieve an expected precise position within 0.01 mm, pressure control is needed. Seeing Figure 10, it has to be noticed that there is a relationship between the intensity of pressure ratio and amplitudes of oscillating mass.

In figure 11, $F_{spring}(t)$ diagrams of PAM in the case of different intensity of pressure ratio can be seen. After damping of oscillation, the spring force in PAM equals the weight of the mass (accurate value: 490.5 N). It is important to notice that by increasing the interval of increase of pressure – similarly to change of amplitudes - the change of spring force in PAM decreases significantly.

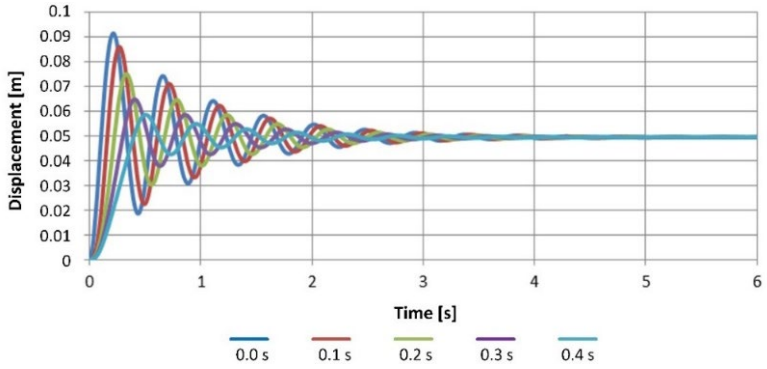

Figure 10
x(t) diagrams of PAM in case of different intensity of pressure ratio

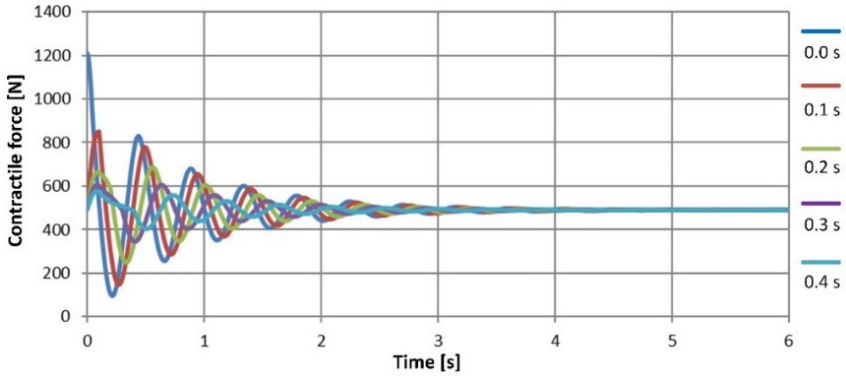

Figure 11

$F_{spring}(t)$ diagrams of PAM in case of different intensity of pressure ratio

4 Simulation of the PAM Dynamics Using the Nonlinear Dynamic Model

Mathematic model (8) of PAM is suitable for positioning by pressure control: initial pressure p_o is adjustable arbitrarily (proposed interval: 0-600 kPa). The change of pressure is controlled by the difference of actual and demanded the position of mass:

$$p_{n+1} = p_n + b(x_{dem} - x) \tag{9}$$

In Equation (9), p_n and p_{n+1} are pressures in PAM after nth, respectively n+1-th time step, b is the intensity factor of pressure ratio, x_{dem} is the demanded position. Finally, x is the actual position of the mass point after nth time step.

3.1. First Task

From position x= 0 mm to lift 10 kg mass by PAM to the demanded level of 40 mm. The initial pressure is p_o= 10^5 Pa; the value intensity factor of pressure ratio is b=0.01. In Figure 12-13, the pressure in PAM and the mass position in the function of time can be seen in a time interval of 0 to 6 seconds.

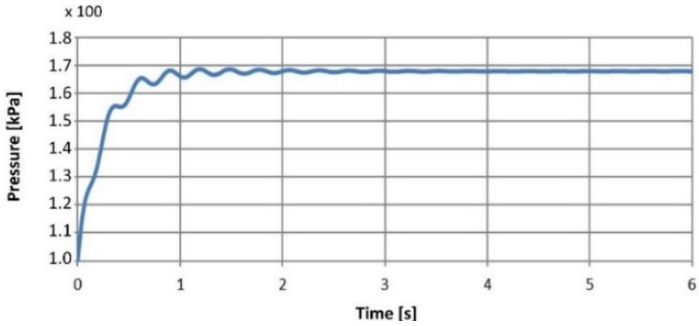

Figure 12
Pressure in PAM in the function of time, position changes from 0 mm to 40 mm

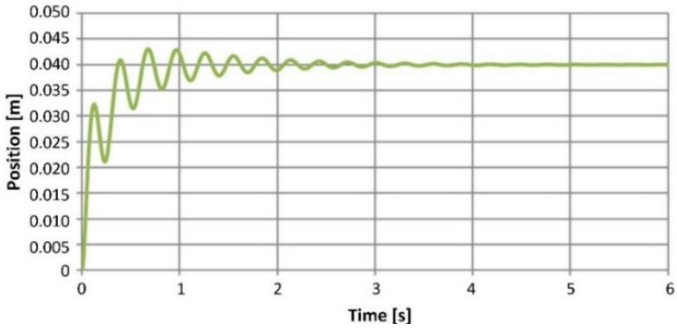

Figure 13
Position of mass in the function of time, position changes from 0 mm to 40 mm

3.2. Second Task

The mass point starts from position x= 40 mm. Its demanded level of 30 mm (Figure 14-15). Initial pressure p_o=1.678 x 100 kPa is needed to keep it at the initial position. The value of the intensity factor of pressure ratio is b=0.012.

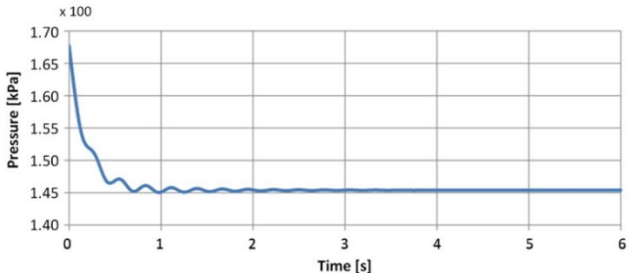

Figure 14
Pressure in PAM in the function of time, position changes from 40 mm to 30 mm

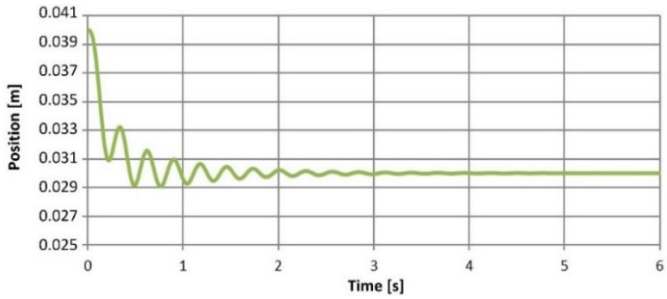

Figure 15
Position of mass in the function of time, position changes from 40 mm to 30 mm

3.3. Third Task

Finally, 25 kg mass starts from position x=0 mm. Its demanded level of 50 mm (Figure 16-17). Initial pressure p_o=2 x 100 kPa. The value of the intensity factor of pressure ratio is b=0.005.

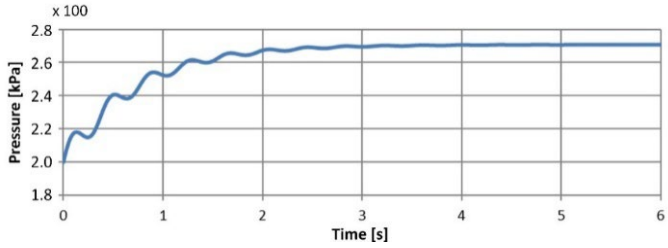

Figure 16
Pressure in PAM in the function of time, position changes from 0 mm to 50 mm

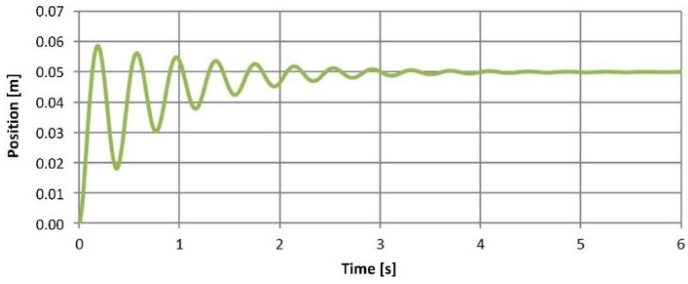

Figure 17
Position of mass in the function of time, position changes from 0 mm to 50 mm

3.4. Subsequent Tasks

To investigate the accuracy of this method, let us study further examples: the pressure to keep 10 kg mass at the level of 50 mm exactly is 1.91768913274509 x 100 kPa. The initial pressure is a little bit lower: p_o=1.91768913274 x 100 kPa (Figure 18). For this reason, the mass point starts downward and, after damping oscillation - as a result of pressure control - stops precisely at the demanded level of 50 mm. The initial and final positions are the same. The temporary disorder is caused by intentionally modified initial pressure.

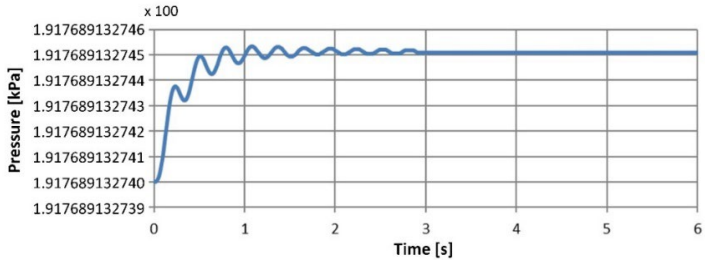

Figure 18
Pressure in PAM in the function of time, initial and final positions are 50 mm

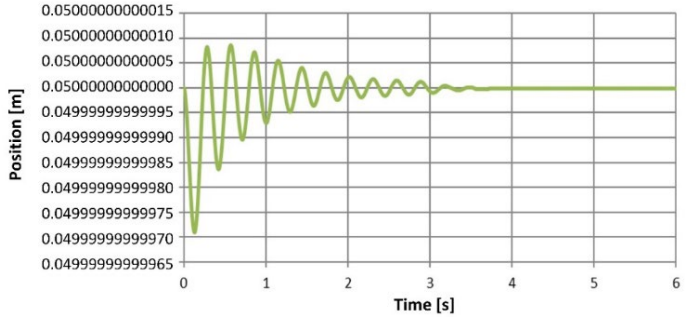

Figure 19
Position of mass in the function of time, initial and final positions are 50 mm

The role of *b* intensity factor of pressure ratio is quite important. Its determination happens empirically in the example above *b*=0.01. If it is modified to 0.005, diagrams are also limited as a result (Figure 20-21). The pressure increase is slower, and the final position is slightly under the one demanded.

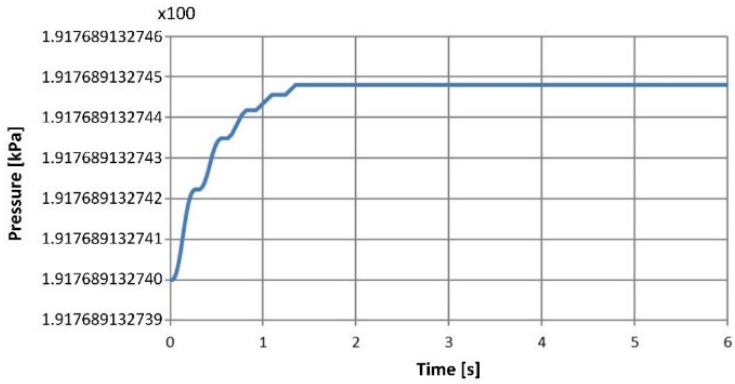

Figure 20

Pressure in PAM in the function of time, the intensity factor of pressure ratio b=0.01

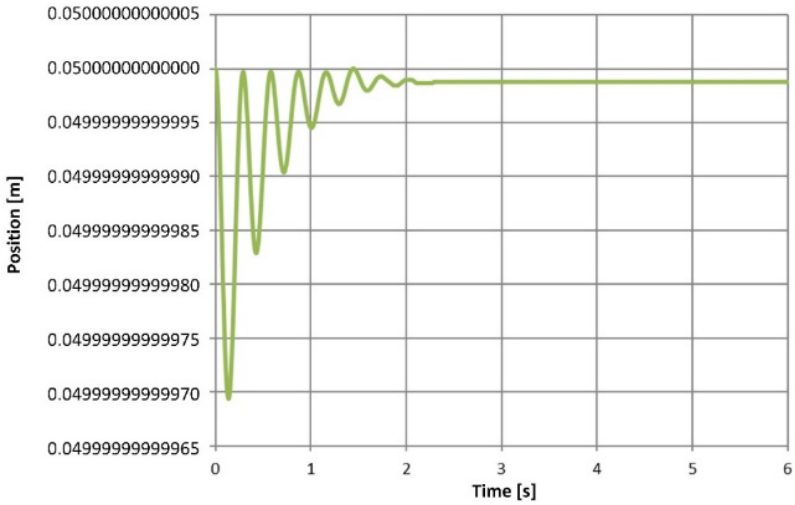

Figure 21

Position of mass in the function of time, the intensity factor of pressure ratio b=0.01

Forms of curves are significantly different when the intensity factor of pressure ratio is b=0.02. In this case, the stimulating effect of pressure changes is stronger than the internal damping action of PAM. Because the pressure change is controlled by the position change of the mass point, it is excited on the natural frequency. Despite damping, the result is similar to phenomena of resonance, but in this case, the amplitude is getting bigger and bigger, exceeding the usual linear connection (Figure 22-23).

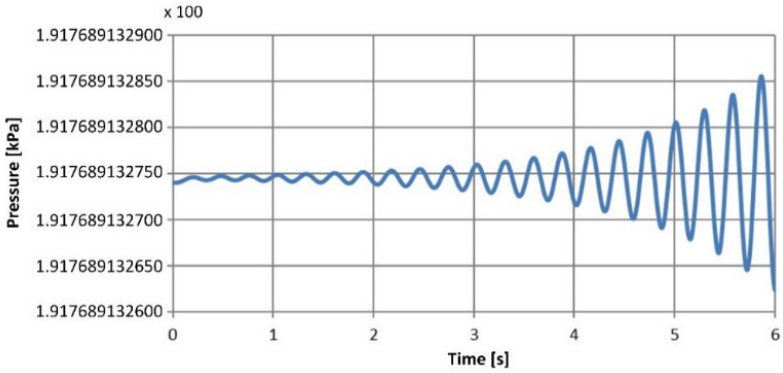

Figure 22
Pressure in PAM in the function of time, the intensity factor of pressure ratio b=0.02

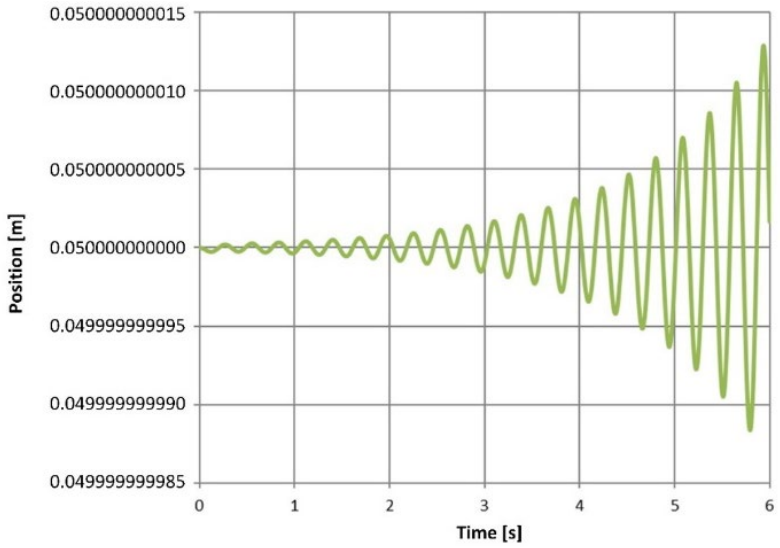

Figure 23
Position of mass in the function of time, the intensity factor of pressure ratio b=0.02

There is a border between the two cases mentioned above when the intensity factor of pressure ratio is b=0.01585. Therefore, the task is to lift a mass m=10 kg from level 49 mm and keep its position on the level of 50 mm. In this case, the amplitudes of excited-damped oscillation in the function of time are the same. The initial pressure p_o=1.91768732075 x 100 kPa is needed to keep the mass point at the level of 50 mm (Figure 24-25).

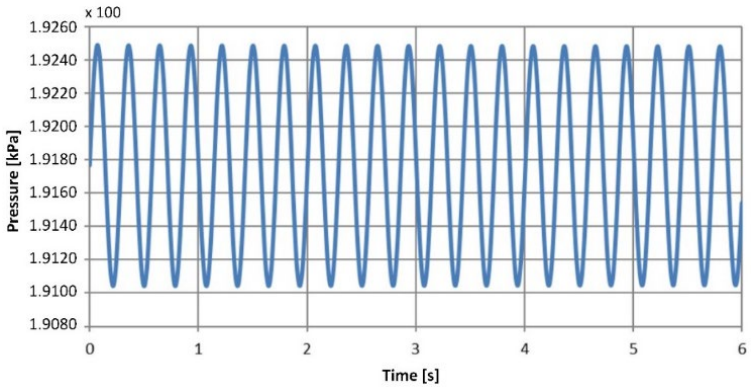

Figure 24

Pressure in PAM in the function of time, the intensity factor of pressure ratio b=0.01585

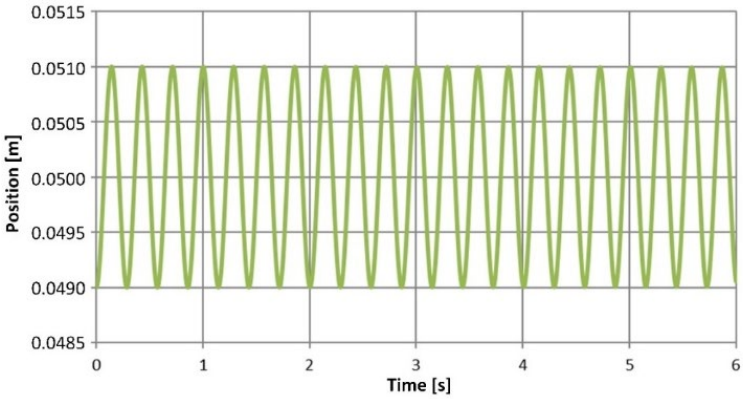

Figure 25

Position of mass in the function of time, the intensity factor of pressure ratio b=0.01585

Conclusions

The presented mathematical model of the vertically mounted nonlinear oscillating system (Figure 1), consisting of mass and excited by in time-variable pressure elastic pneumatic artificial muscle, can take into consideration the change of spring stiffness and damping factor, in the function of contraction, as well as the effect on the oscillation of in time-variable pressure. The value of the pressure and the intensity of its change, significantly affects the dynamic behavior of the weakly damped oscillating system. This mathematical model is suitable for precise and quick positioning, without oscillating different mass points using pressure control. During the pressure control, the following quantities are considered: Position difference of mass points between actual and those demanded, velocity, acceleration and jerk of the mass.

Acknowledgement

The project was supported by the projects VEGA no. 1/0700/20 Object Recognition Techniques with Convolutional Neural Networks and KEGA no. 055TUKE-4/2020 Transfer of knowledge from research on digitization of production processes into study programs of the Faculty of Manufacturing Technologies.

References

[1] Siciliano, B. and Khatib, O.: Springer Handbook of Robotics, *Springer*, 2016, p. 2259

[2] Zhao, J. et al.: Position Control of a Pneumatic Muscle Actuator Using RBF Neural Network Tuned PID Controller, *Mathematical Problems in Engineering*, 2015, pp. 1-16

[3] Ahn, K. K. and Anh, H. P. H.: Comparative Study of Modeling and Identification of the Pneumatic Artificial Muscle (PAM) Manipulator Using Recurrent Neural Networks, *Journal of Mechanical Science Technology*, 2008, Vol. 22, No. 7, pp. 1287-1298

[4] Sárosi, J. et al.: Static Force Model-Based Stiffness Model for Pneumatic Muscle Actuators, *International Journal of Engineering Research in Africa*, 2015, Vol. 18, pp. 207-214

[5] Pitel', J. and Tóthová, M.: Dynamic modeling of PAM based actuator using modified Hill's muscle model, *In Proceedings of the 14th International Carpathian Control Conference (ICCC)*, Poland, May 2013, pp. 307-310

[6] Kang, B.-S. et al.: Dynamic Modeling of Mckibben Pneumatic Artificial Muscles for Antagonistic Actuation, *2009 IEEE International Conference on Robotics and Automation*, Japan, May 2009, pp. 182-187

[7] FESTO Fluidic Muscle DMSP/MAS Available online: https://www.festo.com/rep/en_corp/assets/pdf/info_501_en.pdf (accessed on 10 November 2019.

[8] Wickramatunge, K. C. and Leephakpreeda, T.: Study on Mechanical Behaviors of Pneumatic Artificial Muscle, *International Journal of Engineering Science,* 2010, Vol. 48, No. 2, pp. 188-198

[9] Luo, Z. et al.: Advances in Research on Artificial Muscles Technology and Its Control Algorithm, *In Proceedings of the 2010 2nd International Conference on Advanced Computer Control*, China, March 2010, Vol. 3, pp. 48-51

[10] Davis, S. et al.: Enhanced Modelling and Performance in Braided Pneumatic Muscle Actuators, *I. J. Robotic Res.,* 2003, Vol. 22, pp. 213-228

[11] Kelasidi, E. et al.: A Survey on Pneumatic Muscle Actuators Modeling, *In Proceedings of the 2011 IEEE International Symposium on Industrial Electronics*, Poland, June 2011, pp. 1263-1269

[12] Hošovský, A. et al.: Dynamic Characterization and Simulation of Two-Link Soft Robot Arm with Pneumatic Muscles, *Mechanism and Machine Theory*, 2016, Vol. 103, pp. 98-116

[13] Hošovský, A. and Židek, K.: Experimental Validation of Nominal Model Characteristics for Pneumatic Muscle Actuator, *Applied Mechanics and Materials*, 2014, Vol. 460, pp. 1-12

[14] Wickramatunge, K.C. and Leephakpreeda, T.: Empirical Modeling of Pneumatic Artificial Muscle, *In Proceedings of the Proceedings of the International Multi Conference of Engineers and Computer Scientists (IMECS 2009)*, Hong Kong, March 2009, pp. 1726-1730

[15] Cao, J. et al.: A New Dynamic Modelling Algorithm for Pneumatic Muscle Actuators, *In Proceedings of the Intelligent Robotics and Applications,* 2014; pp. 432-440

[16] Zhang, Z. and Philen, M.: Pressurized Artificial Muscles, *Journal of Intelligent Material Systems and Structures,* 2012, Vol. 23, pp. 255-268

[17] Kothera, C. S. et al.: Experimental Characterization and Static Modeling of McKibben Actuators, *Journal of Mechanical Design*, 2009, Vol. 131, pp. 1-10

[18] Takosoglu, J. E. et al.: *Determining the Static Characteristics of Pneumatic Muscles, Measurement and Control*, 2016, Vol. 49, pp. 62-71

[19] Doumit, M. et al.: Analytical Modeling and Experimental Validation of the Braided Pneumatic Muscle, *IEEE Transactions on Robotics,* 2009, Vol. 25, No. 6, pp. 1282-1291

[20] Tóthová, M. et al.: Numerical Approximation of Static Characteristics of Mckibben Pneumatic Artificial Muscle, *International Journal of Mathematics and Computers in Simulation*, 2015, Vol. 9, pp. 228-233

[21] Sarosi, J. et al.: Dynamic Modeling of a Pneumatic Muscle Actuator with Two-Direction Motion, *Mechanism and Machine Theory*, 2015, Vol. 85, pp. 25-34

[22] Doumit, M. D. and Pardoel, S.: Dynamic Contraction Behaviour of Pneumatic Artificial Muscle, *Mechanical Systems and Signal Processing*, 2017, Vol. 91, pp. 93-110

[23] Kalita, B. and Dwivedy, S. K.: Nonlinear Dynamics of a Parametrically Excited Pneumatic Artificial Muscle (PAM) Actuator with Simultaneous Resonance Condition, *Mechanism and Machine Theory*, 2019, Vol. 135, pp. 281-297

[24] Ito, A. et al.: Motion Control of Parallel Manipulator Using Pneumatic Artificial Actuators, *In Proceedings of the 2010 IEEE International Conference on Robotics and Biomimetics*, China, December 2010, pp. 460-465

[25] Tondu, B.: Modelling of the McKibben Artificial Muscle: A Review, *Journal of Intelligent Material Systems and Structures,* 2012, Vol. 23, pp. 225-253

[26] Sárosi, J.: Elimination of the Hysteresis Effect of PAM Actuator: Modelling and Experimental Studies, *Tehnički vjesnik*, 2015, Vol. 22, No. 6, pp. 1489-1494

[27] Aschemann, H. and Schindele, D.: Comparison of Model-Based Approaches to the Compensation of Hysteresis in the Force Characteristic of Pneumatic Muscles, *IEEE Transactions on Industrial Electronics*, 2014, Vol. 61, No. 7, pp. 3620-3629

[28] Al-Ibadi, A. et al.: Valuable Experimental Model of Contraction Pneumatic Muscle Actuator, *In Proceedings of the 2016 21st International Conference on Methods and Models in Automation and Robotics (MMAR)*, Poland, August 2016, pp. 744-749

[29] Gaiser, I. et al.: Compliant Robotics and Automation with Flexible Fluidic Actuators and Inflatable Structures, *In INTECH,* 2012, pp. 567-608

[30] Laski, P. A. et al.: Design of a 3-DOF Tripod Electro-Pneumatic Parallel Manipulator, *Robotics and Autonomous Systems,* 2015, Vol. 72, pp. 59-70

[31] Bleicher, A. et al.: Model-Based Design and Experimental Validation of Active Vibration Control for a Stress Ribbon Bridge Using Pneumatic Muscle Actuators, *Engineering Structures,* 2011, Vol. 33, No. 8, pp. 2237-2247